International Journal of Electrical, Electronic and Communication Sciences
ISSN: 2517-9438
Vol:11, No:2, 2017

sEMG Interface Design for Locomotion Identification

Rohit Gupta, Ravinder Agarwal

***Abstract*—**Surface electromyographic (sEMG) signal has the potential to identify the human activities and intention. This potential is further exploited to control the artificial limbs using the sEMG signal from residual limbs of amputees. The paper deals with the development of multichannel cost efficient sEMG signal interface for research application, along with evaluation of proposed class dependent statistical approach of the feature selection method. The sEMG signal acquisition interface was developed using ADS1298 of Texas Instruments, which is a front-end interface integrated circuit for ECG application. Further, the sEMG signal is recorded from two lower limb muscles for three locomotions namely: Plane Walk (PW), Stair Ascending (SA), Stair Descending (SD). A class dependent statistical approach is proposed for feature selection and also its performance is compared with 12 preexisting feature vectors. To make the study more extensive, performance of five different types of classifiers are compared. The outcome of the current piece of work proves the suitability of the proposed feature selection algorithm for locomotion recognition, as compared to other existing feature vectors. The SVM Classifier is found as the outperformed classifier among compared classifiers with an average recognition accuracy of 97.40%. Feature vector selection emerges as the most dominant factor affecting the classification performance as it holds 51.51% of the total variance in classification accuracy. The results demonstrate the potentials of the developed sEMG signal acquisition interface along with the proposed feature selection algorithm.

***Keywords*—**Classifiers, feature selection, locomotion, sEMG.

I. Introduction

SURFACE electromyography (sEMG) signals have a paramount importance and potential in the field of robotics, it is widely applied to control assistive and rehabilitative devices like prosthetics, exoskeletons, wheelchairs etc. The controlling of such devices is done by identifying the insight information in the signal [1]. To exploit the above-mentioned property of the sEMG signal many industries developed sophisticated and high cost sEMG measuring instruments like Nexus 10, Trigno etc. Many research groups have developed their own sEMG interface systems for laboratory use [2]–[4]. Earlier developed systems exploited instrumentation amplifiers e.g. AMP04FPZ, INA114, INA128P as a component [4]–[6], but the major disadvantage is that, for each channel one dedicated IC is used, which increase the component bourdon on developed instrument. Some of the researchers proposed active electrode system and systems with lesser circuitry [7], [8] but in these systems dedicated cables and interface increase the cost of the system.

The hidden information in the sEMG signal is treated as feature of a particular signal, so that after signal acquisition, the appropriate signal processing techniques need to be applied, a trade off should be made between information loss and excess/vague information retention. Loss in information carried by the signal degrade the quality of the signal, such as the identification of functionality in the signal; whereas the excess information acts as noise that will ultimately retrench the performance of the system [9]. In the recent past, various researchers have applied different combinations of extracted features and pattern recognition algorithms and post-processing techniques for the application of activity recognition of both upper and lower limbs [1], [3], [10]–[12]. The features utilized by previous researchers are mainly from the time domain, frequency domain and time-frequency domain (wavelet transform). Out of these three domains, the time domain based features gained popularity, as these are computationally inexpensive, easy to implement and provide better results [13]–[17]. Multiple studies had been performed by various researchers on activity identification using sEMG signal or mechanical sensors or both, and the majority of them are on upper limb activity identification [18], but in past couple of decades, recognizable work had been done on lower limb activity recognition also. Major studies of locomotion identification are summarized in Table I. Table I shows that very few studies on particular application are conducted using sEMG signal and also these studies used multiple muscles signals along with a higher number of features. Still there is lot of scope to exploit sEMG signal for the current application.

In this paper, a single muscle based continuous locomotion identification approach was explored. Here, sEMG signal from two lower limb muscles was recorded during three types of locomotion namely: Plane Walk (PW), Stair Ascending (SA), Stair Descending (SD). To acquire the sEMG signal, ADS1298 IC based sEMG interface was developed. Twelve feature vectors were constructed using 38 features (time and frequency domain) extracted from the recorded signal and classification performance of five different types of classifiers namely; Decision Tree (DT), k-Nearest Neighbor (KNN), Artificial Neural Network (ANN), Support Vector Machine (SVM) and Linear Discernment Analysis (LDA) were compared for all feature vectors. Also, a class dependent statistical based approach of feature selection was proposed and compared. All the results were compared subject-wise to analyze the variation in performance.

Rohit Gupta is with the EIED, Thapar University, Patiala, Punjab, India (e-mail: rohit.gupta@ thaapr.edu).

Ravinder Agarwal is with the EIED, Thapar University, Patiala, Punjab, India (corresponding author, phone: 01752393062, e-mail: ravinder_eeed@ thaapr.edu).

TABLE I
MAJOR STUDIES ON LOCOMOTION IDENTIFICATION

	No. of Muscles	No. of features	Classifier	Max. acc.
Only mechanical senor				
[19]	**	52	LDA	97%
[20]	**	22	Phase Dependent LDA, QDA, LR	93%
[21]	**	52	LDA	84.5%
[22]	**	59	Phase dependent LDA	98.4%
[23]	**	5	Phase dependent classifier	98%
[24]	**	6	Locomotion dependent LDA	88%
Only sEMG signal				
[25]	3	24	LDA, ANN, NBC	95%
[26]	11	11	Phase dependent LDA	95%
[27]	12	36x45	LDA, SVM, NN	90%
Both mechanical sensor and sEMG signal				
[28]	11	88	Phase dependent NB	100%
[29]	7	28	LDA	97%
[30]	9	36	Phase dependent LDA	98%
[13]	4	60	LDA, SVM	97%
[31]	8	86	Phase dependent SVM	95%
[32]	9	99	Phase dependent LDA	98%
[33]	9	124	LDA, NB	98%
[34]	7	987	LDA, SVM	84%

II. MATERIAL AND METHODS

A. sEMG Signal Acquisition Interface Design

The basic modules needed to design an sEMG based activity recognition system are shown in Fig. 1.

The circuit diagram to interface ADS1298 IC is shown in Fig. 2 [35]. Disposable, self-adhesive silver/silver chloride (Ag/AgCl) snap electrodes having two circular conductive areas of 1.0 cm each and an inter-electrode distance of 2.0 cm were used to pick up the electrical signal from the human body during activity. A Schottky diode protection circuit was utilized for over voltage protection and a second order RC filter of cutoff frequency 1000Hz was used for each channel. Thereafter, to amplify the signal, a programmable gain amplifier was used, with a gain of 1000. Further, the amplified signal was converted into a digital signal to transfer it to the processing device. The amplification and analog to digital conversion was performed through one ADS1298 IC. There are many more advantages of using ADS1298 IC for such a type of system development, some of them are [36]; i) power decapitation of device goes down, ii) complexity of the system reduced, iii) cost of the system reduced, iv) due to single pin output of ADC for eight pin input, modularity of the system increased, v) sensitivity of the ADC can be varied at the programming level, vi) sampling frequency can be modified as per requirement, vii) lead off protection is provided which can be used for a safety feature, viii) programmable, adjustable gain provides the flexibility of choosing different gains.

To transfer the digital output of the ADS1298 in the processing device, an interfacing programmable device was used with the SPI protocol enabled pin. For this system, a Teensy 3.2 module was used, which is small in size and powered through the same power supply used for the ADS1298. The output (sEMG signal) of Teensy 3.2 was transferred and saved in a personal computer through serial communication that was further processed and analyzed using MATLAB 2015a.

The proposed eight channels sEMG interface cost less than 5,000 INR (approximately US$73), whereas commercially available standard multichannel sEMG signal acquisition system costs more than 200,000 INR (approximately US$2,900). Further, there is no need to procure any recording cables and any other interfacing device like a DAQ card or others. Here, signals were sampled at 2024 samples/sec and all other offline signal processing was done in Intel core i3 personal computer with 2.53 GHz and 3.80 GB of RAM.

B. Data Collection and Signal Processing

Five subjects having normal gait walk participated in the experimental study. Two muscles, the Fibularis longus (below the knee) M1 and Biceps Femoris (above the knee) M2 were used for the sEMG signal recording. These muscles were selected due to; ease of accessibility for the sEMG electrode placement, lower muscle mass, sustainable sEMG signal strength, etc.

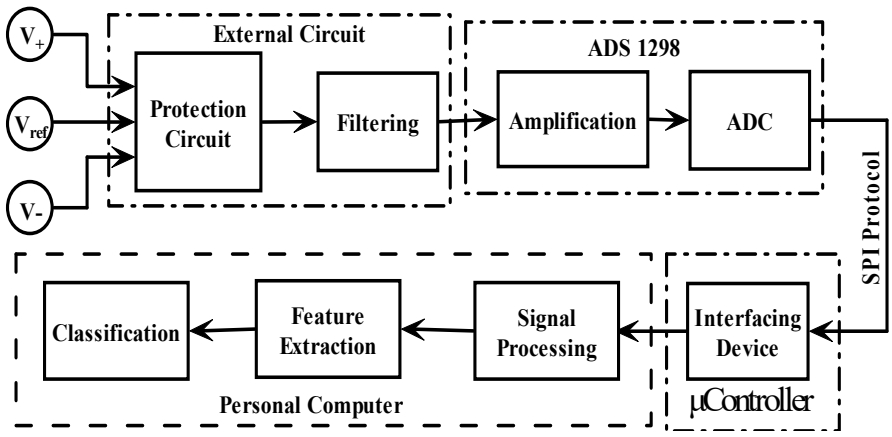

Fig. 1 Basic modules for sEMG based classification system

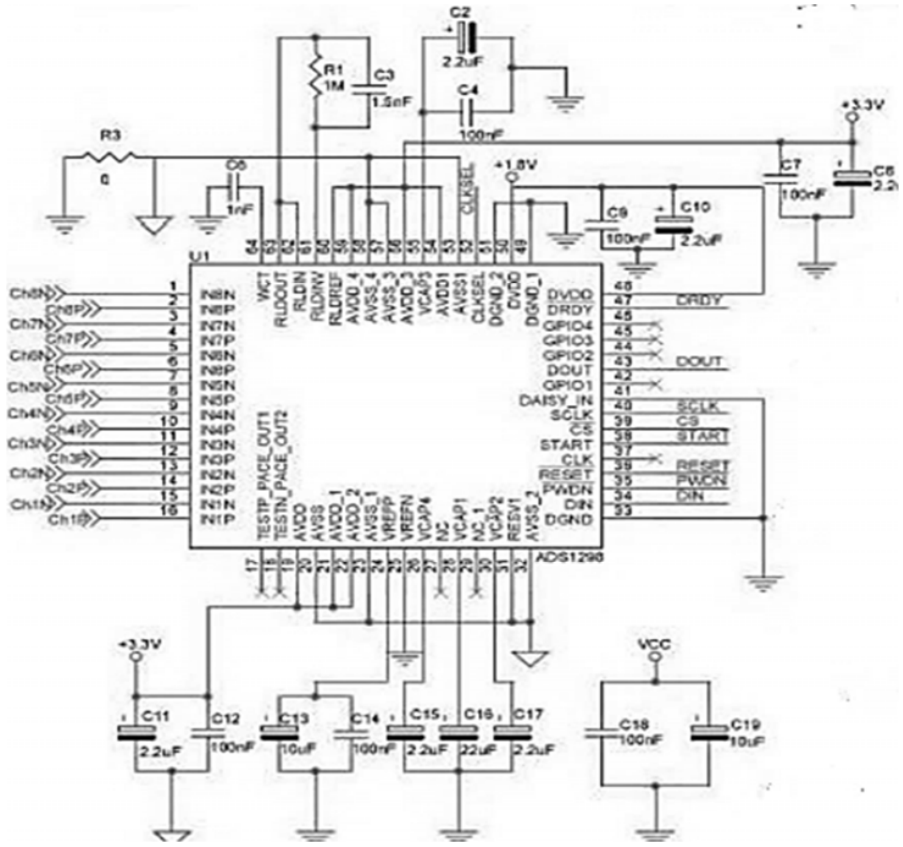

Fig. 2 ADS1298 IC connection diagram

In this study, three major locomotions of daily life were considered PW, SA and SD. Each subject was trained for five trails in each locomotion to maintain their walking speed normal and minimize the cognitive efforts. Five samples of each locomotion were recorded, each recorded sample contains five gait cycles after 20 minutes rest. To avoid muscle fatigue, 20 minutes of resting time was provided after each locomotion sample recording. The recorded signal for muscle 1 during Plain Walking (PW) is shown in Fig. 3.

The recorded sEMG signal was further processed offline; the steps needed are shown in Fig. 4. Filtering and segmentation or windowing of signal was done before extracting the features. For Filtering 4th order band pass butterworth filter, having frequency range of 60-500Hz, was applied [13].

sEMG signal was segmented in multiple windows before feature extraction (Fig. 5). Overlapped windowing techniques was applied which shows the promising results [37]–[41]. Machine learning algorithms show higher classification accuracy for window size between 200 ms to 300 ms [42], for the current research work window length of 256 ms with a shift of 32 ms was used.

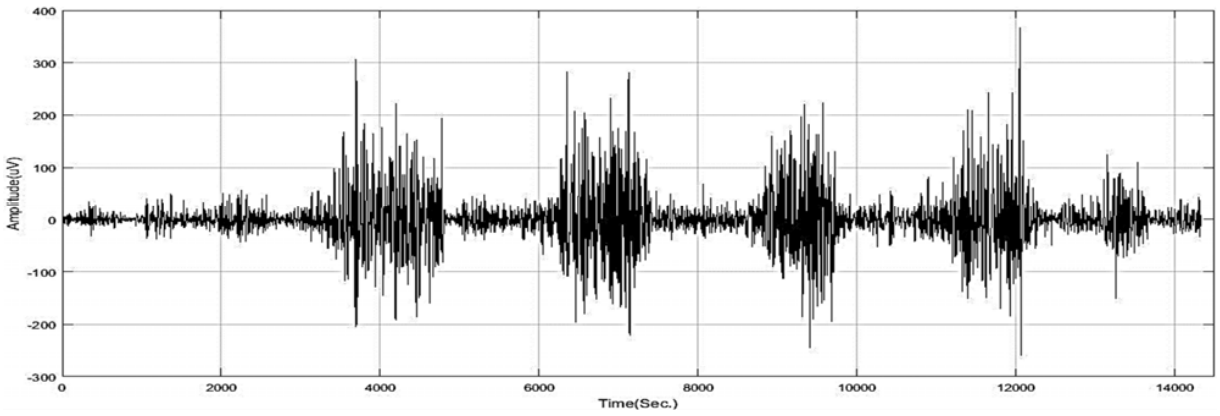

Fig. 3 Recorded sEMG signal for muscle 1 during PW

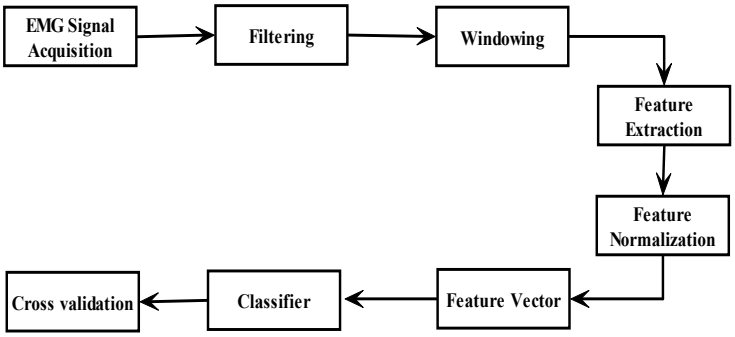

Fig. 4 Block diagram for signal processing

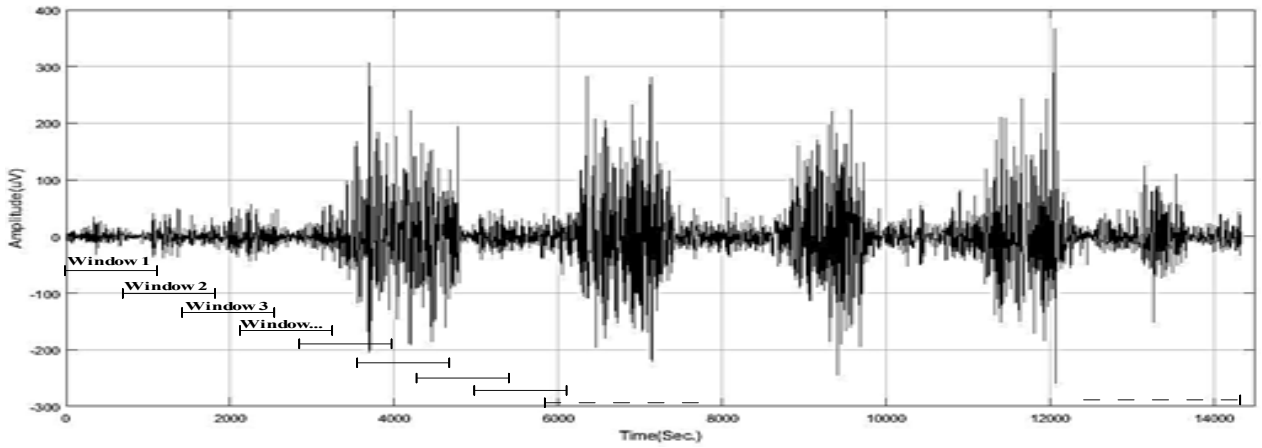

Fig. 5 Segmentation process of sEMG signal

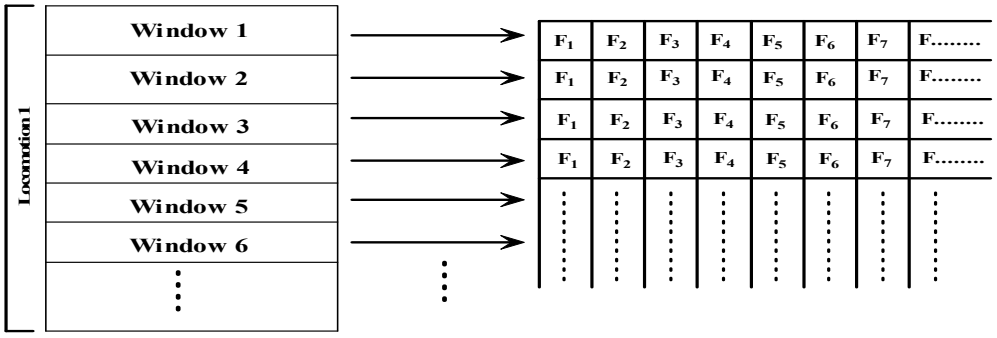

Fig. 6 Feature vector generation for each segment

Each segment of a signal was considered as a training set, the feature vector for each segment was formulated as shown in Fig. 6.

In this study, a total 38 features were extracted which includes time domain and frequency domain features presented in appendix (A1). Min-max normalization method was used to normalize the features individually to enhance the performance of classifier [43]. Further, these normalized features were grouped according to mathematical properties and information into 12 groups (Table II).

C. Classifiers and Performance Evaluation

The selection of the classifier is also an important factor which depends on available/training data type and application. Here, five different types of classifiers, SVM, LDA, ANN, DT and KNN were compared for the application of locomotion identification.

To validate the classifier performance, repeated k-fold cross validation scheme was used. In k-fold cross validation scheme, the complete data was divided into k separate parts, out of which k-1 parts were used to train the classifier and only one part to test the classifier. To check the scheme regress, k-fold validation was repeated multiple times. Therefore, 10-fold cross validation was repeated 100 times and the average of that was used as representative performance. The performance measure was quantified as

overall % accuracy (1).

$$\%Acc = \frac{No.of\ correctly\ classified\ testing\ data}{Total\ no.of\ applied\ testing\ data} X100\% \quad (1)$$

TABLE II
FEATURE VECTOR INFORMATION

Abv./ No of features	Features in feature vector	Vector methodology
TD/23	All time domain features	Features having time domain information
FD/11	All frequency domain features	Features having frequency domain information
AR/4	AR1, AR2, AR3, AR4	Predictive information based features
TFD/34	All time and frequency domain features	All time and frequency domain features
TAD/27	All time and predictive domain features	Time and predictive information based features
FAD/15	All frequency and predictive domain features	Frequency and predictive information based features
TFAD/38	All time, frequency and predictive domain features	Time, frequency and predictive information based features
HuF/4	MAV, WL, ZC, SSC	Hudgin's feature vector [44]
DuF/6	IEMG, VAR, WL, ZC, SSC, WAMP	Du's feature vector [45]
EnF/8	IEMG, MAV, MAV1, MAV2, SSI, VAR, RMS, LOG	Features having energy information
CoF/6	WL, AAC, DASDV, TM3, 4, 5	Complexity information based features
FITD/4	ZC, MYOP, WAMP, SSC	Features having frequency information in time domain
CSF/16	SSI, VAR, TM3, 4, 5, DASDV, H1,2,4,5, MNF, MDF, PKF, FR, PSR, VCF, AR4	Class dependent statistical approach *(proposed)*

III. PROPOSED FEATURE SELECTION ALGORITHM

The performance of any classifier is highly dependent on information used for the training of classifier. The redundant information/features were avoided as these redundant features act as noise and the classifiers suffers from over fitting. The steps involved in the proposed method (for three activities) for a class dependent statistical approach are as follows:

Step 1. Record the training data class wise.
Step 2. Extract the features from the training data.
Step 3. Consider one feature at a time:
i. Arrange the data in all possible combinations/groups pair of activities (1&2, 2&3 and 3&1);
ii. Apply one way ANOVA analysis to check whether the feature have significant difference in between activity; and,
iii. Store the p values of feature w.r.to activity combinations.
Step 4. Repeat step 3 for each feature *(after this step, users have three p value for each feature corresponding to pair of activities combinations).*
Step 5. Rank each feature as per their p value, the smaller the p value, the higher the ranking *(after this step, users have three ranks for each feature corresponding to pair of activities combinations).*
Step 6. Select the top performing features (lower p values, $p<0.001$) from each group and generate feature vector *(common features in more than one group will be considered ones).*

The basic methodology applied for feature selection was to rank the individual feature as per their ability to distinguish between pair of activities, for that p value was considered *(lower the p value higher the distinguishability)*. To check the p value of each feature one way ANOVA analysis was performed for individual feature. Thereafter, features having $p<0.001$ from all pair of activities group put together to construct feature vector. Total of 16 features were selected out of 38 features and most of them are time domain features.

IV. RESULTS AND DISCUSSION

A. Effect of Subject Variability on Classification Accuracy

To determine the effect of subject variability on classification accuracy, one-way analysis of variance (ANOVA) test was performed on each classifier individually for both the muscles.

Table III shows the p-values obtained for each classifier and muscles.

TABLE III
P-VALUES FOR ONE WAY ANOVA

Sr. No.	Classifier	Muscle 1	Muscle 2
1.	SVM	0.85	0.50
2.	LDA	0.09	0.09
3.	NN	0.50	0.06
4.	DT	0.76	0.0009
5.	KNN	0.89	0.0001

It was observed that subject variability does not have a statistically significant effect on classifiers performance as for all the classifies the obtained p value > 0.05, only DT and KNN classifiers have significant difference in classifier performance with respect to subjects. To reduce the complexity of problem from comparison point of view, classification performance was averaged over the five subjects for further analysis.

B. Effect of Muscle Variability on Classification Accuracy

To determine the effect of muscle variability on classification accuracy, one-way analysis of variance (ANOVA) test was performed on each classifier individually. The subject variation was removed by averaging the classification performance. Over all second muscle performs better if all the feature vectors were given same weightage, as illustrated in Fig. 7.

C. Feature Vector & Classifier Performance

Table IV illustrates the classification performance of various classifiers for each feature vector. Top 50% best performing feature vectors are highlighted for each classifier. The major top performing feature vectors are TD, FD, TFD, TAD, FAD, TFAD and CSF for all the classifiers.

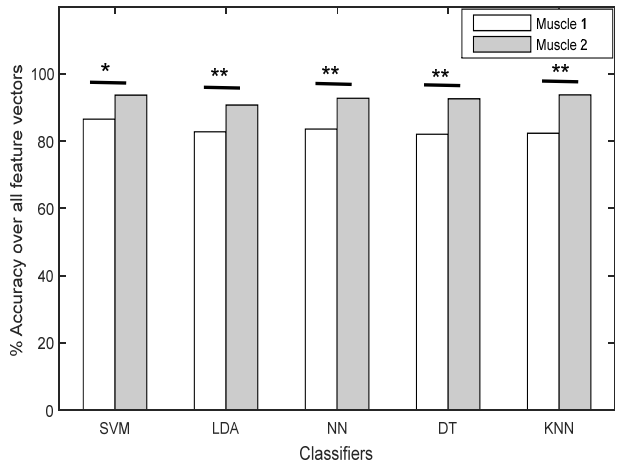

Fig. 7 Averaged classification accuracy of various classifiers for both the muscles *(* p-value<0.01, ** p-value<0.001)*

For the SVM classifier and muscle 1, the TD feature vector performs best (98.79±0.37), as compared to the other feature vectors, while CSF was the second best (98.73±0.68) performing feature vector. In order to test the significance of classification accuracy, ANOVA test was applied with a significance level of 0.01. The ANOVA test shows no significant difference in performance of TD and CSF. For muscle 2, TD was the best (98.73±0.53) performing feature vector, whereas TFD, TAD were the second best (97.84±0.94), (97.84±0.72) performing feature vectors and ANOVA test showed no significant difference in performance with significance level of 0.01.

For the LDA classifier, the results show that the TAFD and TFD feature vectors performed best (99.65 ± 0.36 for muscle 1 and 99.05 ± 0.42 for muscle 2), and second best (98.32 ± 0.53 for muscle 1 and 97.84 ± 0.60 for muscle 2), and for both the muscles, the ANOVA test also showed a significant difference in classification accuracy with significance level of 0.01. For the NN classifier, the results of muscle 1 demonstrates the TFAD feature vector as the best (98.73 ± 0.82) performing feature vector and CSF as the second best (97.08 ± 1.97) performing feature vector with statistically significant difference with a significance level of 0.01; whereas for muscle 2, TFAD (97.94±0.63) and TD (96.89±1.02) were the best and second best performed feature vectors, but with no statistically significant difference. Similarly, the results shown for classifier DT and KNN were interpreted.

TABLE IV
PREDICTIVE PERFORMANCE (%CLASSIFICATION ACCURACY) OF CLASSIFIERS FOR DIFFERENT FEATURE VECTORS

	SVM		LDA		NN		DT		KNN	
	M1	**M2**	**M1**	**M2**	**M1**	**M2**	**M1**	**M2**	**M1**	**M2**
TD	98.79±0.37	98.73±0.53	96.29±1.06	97.14±0.49	97.05±1.35	96.89±1.02	93.78±1.26	93.87±0.52	92.06±1.35	97.02±0.52
FD	97.05±0.65	94.98±1.14	88.35±2.11	90.13±1.75	82.54±7.53	93.14±2.88	91.17±1.75	93.68±1.23	90.41±1.14	95.78±1.23
AR	70.16±2.69	89.87±1.73	67.49±3.52	85.71±2.79	68.03±2.24	89.21±1.84	63.81±5.85	92.76±1.52	68.79±2.80	92.38±1.52
TFD	96.54±1.13	97.84±0.94	98.32±0.53	97.84±0.60	95.62±2.00	96.29±1.16	84.13±5.02	93.24±1.23	89.21±1.82	94.92±1.23
TAD	96.86±0.98	97.84±0.72	96.86±0.76	97.11±0.93	95.81±1.55	96.44±1.91	93.43±1.38	94.32±1.26	83.59±1.42	92.41±1.26
FAD	98.57±0.65	95.65±0.82	93.27±1.93	90.86±1.78	96.35±2.38	94.38±1.65	91.40±1.32	93.68±1.52	94.92±0.55	95.05±1.52
TFAD	97.24±1.00	97.75±0.71	99.65±0.36	99.05±0.42	98.73±0.82	97.94±0.63	90.19±1.60	93.78±0.86	91.62±0.92	96.03±0.866
HuF	69.84±2.00	88.73±1.81	66.79±3.09	86.25±2.40	68.00±2.47	89.02±1.80	66.41±2.34	87.71±1.60	67.97±2.68	91.24±1.60
DuF	74.57±1.76	89.87±1.42	69.24±3.07	85.33±2.04	73.37±3.77	89.56±1.78	71.97±1.84	92.95±1.21	75.94±1.35	92.63±1.21
EnF	81.90±1.46	90.67±2.1	70.67±2.26	85.46±2.22	73.17±5.36	89.14±2.33	91.05±1.62	93.21±1.44	81.11±1.70	92.57±1.44
CoF	74.57±2.99	90.06±2.19	69.17±2.67	85.59±1.97	71.46±3.62	89.59±1.67	72.60±2.62	92.51±1.79	76.16±2.48	92.41±1.79
FITD	69.87±1.83	88.73±1.81	67.27±3.40	86.25±2.4	67.49±1.81	89.02±1.80	65.65±2.34	87.71±1.60	67.84±1.74	91.24±1.60
CSF	98.73±0.68	96.98±0.59	92.38±2.20	92.63±1.82	97.08±1.97	94.95±1.93	90.70±1.96	94.16±1.25	90.70±1.78	94.73±1.25

The results shown by the classifiers, possess quit variability in terms of best performing feature vectors. Feature vectors having a maximum number of features did not perform best for each classifier, which reflects the variability and unique nature of the classifiers. So, for each classifier, comparative analysis is necessary in order to find a suitable feature vector. One common reflection made by all classifiers was that feature vectors having time domain features performs comparatively better, which suggests one should pay more attention towards time domain based features. The feature vector (CSF) selected through the proposed feature selection algorithm stood well against other feature vectors in terms of performance and number of features. But, there is still scope for improvement in the feature selection algorithm, and the presented results suggest including the variability of the classifiers with the feature vector selection algorithm.

To identify the best performed classifier, the predictive performance of the top 50% feature vectors was averaged over the feature vector and muscles as well; the result is shown in Fig. 8. The SVM classifier possess the best accuracy as compared to other classifiers, whereas ANOVA test shows all the classifier pairs performed statistically similarly for the top 50% selected feature vectors, apart from the classifier pair SVM and DT.

To quantify the effects of experimental factors (Feature vector, Muscle and classifier), a multifactor analysis of variance (ANOVA) on classification accuracy was performed. It was observed that all three experimental factors and their interactions were the significant factors affecting the prediction performance, as their p-value was <0.01 for

significance level 0.01. Fig. 9 shows that feature vector is the most dominant source of variability with 51.51% of total variance in classification accuracy. Muscle selection also plays an important role, as it possesses 20.83% of total variance. Whereas classifier selection illustrates the least percentage variance (1.26%) among the three compared experimental factors.

V. Conclusion

In this paper, a low cost multichannel sEMG interface for clinical and research laboratory purpose was developed. The developed interface utilized ADS1298 integrated circuit, which reduces the problem of existing interfaces like high cost, power combustion and complex circuitry burden. It provides the flexibility to modify the gain of amplifier and sensitivity of ADC without making any change in the circuitry. Further, to prove the suitability and applicability of the developed interface, it was used to acquire the lower limb sEMG signal from two muscles for three locomotions. A comparative study is presented for locomotion identification. The study provides a regress comparison of multiple factors like feature vectors, muscle, classifiers along with class dependent statistical approach of feature selection. The presented results revel that muscle 2 Biceps Femoris (above the knee) performs better for locomotion identification. Also, time domain based features prove their suitability for current application, while multifactor analysis of variance (ANOVA) analysis suggests that classifier selection has least variability in terms of classification accuracy, whereas feature vector selection possesses the most. The potential outcomes of the presented research work will be useful in future for prosthesis control.

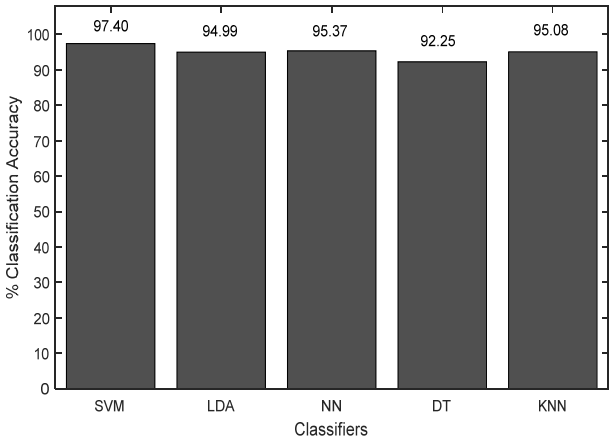

Fig. 8 Classification accuracy for different classifiers over selected feature vectors

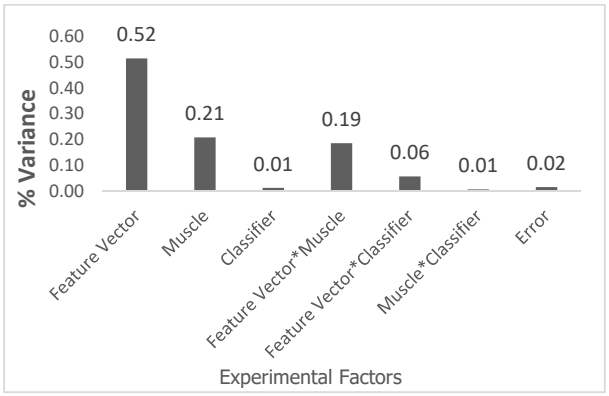

Fig. 9 Variance of classification accuracy shared by experimental factors and their interaction

Appendix

TABLE V
Name and Definition of Extracted Features [9]

Sr. No.	Abv.	Name of Feature	Definition
1	IEMG	Integrated EMG	$IEMG = \sum_{i=1}^{N} \lvert X_i \rvert$
2	MAV	Mean absolute value	$MAV = \frac{1}{N} \sum_{i=1}^{N} \lvert X_i \rvert$
3	MAV1	Modified mean absolute value type 1	$MAV1 = \frac{1}{N} \sum_{i=1}^{N} w_i \lvert X_i \rvert, w_i = \begin{cases} 1 \; if \; 0.25N \le i \le 0.75N \\ 0.5 \; otherwise \end{cases}$
4	MAV2	Modified mean absolute value type 2	$MAV2 = \frac{1}{N} \sum_{i=1}^{N} w_i \lvert X_i \rvert, w_i = \begin{cases} 1 \; if \; 0.25N \le i \le 0.75N \\ \frac{4i}{N} \; elseif \; i < 0.25N \\ \frac{4(i-N)}{N} \; otherwise \end{cases}$
5	SSI	Simple square integral	$SSI = \sum_{i=1}^{N} X_i^2$
6	VAR	Variance of EMG	$VAR = \frac{1}{N-1} \sum_{i=1}^{N} X_i^2$
7	TM3	Absolute value of the 3rd temporal moment	$TM3 = \left\lvert \frac{1}{N} \sum_{i=1}^{N} X_i^3 \right\rvert$
8	TM4	Absolute value of the 4th temporal moment	$TM4 = \left\lvert \frac{1}{N} \sum_{i=1}^{N} X_i^4 \right\rvert$

Sr. No.	Abv.	Name of Feature	Definition
9	TM5	Absolute value of the 5th temporal moment	$TM5 = \left\lvert \frac{1}{N}\sum_{i=1}^{N} X_i^5 \right\rvert$
10	RMS	Root mean square	$RMS = \sqrt{\frac{1}{N}\sum_{i=1}^{N} X_i^2}$
11	LOG	Log detector	$LOG = e^{\frac{1}{N}\sum_{i=1}^{N}\log(\lvert X_i\rvert)}$
12	WL	Waveform length	$WL = \sum_{i=1}^{N-1} \lvert X_{i+1} - X_i\rvert$
13	AAC	Average amplitude change	$AAC = \frac{1}{N}\sum_{i=1}^{N-1} \lvert X_{i+1} - X_i\rvert$
14	DASDV	Difference absolute standard deviation value	$DASDV = \sqrt{\frac{1}{N-1}\sum_{i=1}^{N-1}(X_{i+1} - X_i)^2}$
15	ZC	Zero crossing	$ZC = \sum_{i=1}^{N-1}[sgn(X_i \times X_{i+1}) \cap \lvert X_i - X_{i+1}\rvert \geq threshold]$ $sgn(X) = \begin{cases} 1, if\ X \geq thrsehold \\ 0, otherwise \end{cases}$
16	MYOP	Myopulse percentage rate	$MYOP = \frac{1}{N}\sum_{i=1}^{N}[f(X_i)]$ $f(X) = \begin{cases} 1, if\ X \geq threshold \\ 0, otherwise \end{cases}$
17	WAMP	Willison amplitude	$WAMP = \sum_{i=1}^{N-1}[f(\lvert X_n - X_{n+1}\rvert)]$ $f(X) = \begin{cases} 1, if\ X \geq threshold \\ 0, otherwise \end{cases}$
18	SSC	Slope sign change	$SSC = \sum_{i=2}^{N-1}[f[(X_i - X_{i-1}) \times (X_i - X_{i+1})]]$ $f(X) = \begin{cases} 1, if\ X \geq threshold \\ 0, otherwise \end{cases}$
19	H1		
20	H2		
21	H3	Histogram of EMG	Histogram of EMG
22	H4		
23	H5		
24	MNF	Mean frequency	$MNF = \sum_{j=1}^{M} f_j P_j \Big/ \sum_{j=1}^{M} P_j$
25	MDF	Median frequency	$\sum_{j=1}^{MDF} P_j = \sum_{j=MDF}^{M} P_j = \frac{1}{2}\sum_{j=1}^{M} P_j$
26	PKF	Peak frequency	$PKF = \max(P_j), j = 1, 2 \ldots\ldots, M$
27	MNP	Mean power	$MNP = \frac{\sum_{j=1}^{M} P_j}{M}$
28	TTP	Total power	$TTP = \sum_{j=1}^{M} P_j = SM0$
29	SM1	1st Spectral moments	$SM1 = \sum_{j=1}^{M} P_j f_j$
30	SM2	2nd Spectral moments	$SM2 = \sum_{j=1}^{M} P_j f_j^2$
31	SM3	3rd Spectral moments	$SM3 = \sum_{j=1}^{M} P_j f_j^3$
32	FR	Frequency ratio	$FR = \sum_{j=LL}^{UL} P_j \Big/ \sum_{j=LH}^{UH} P_j$
33	PSR	Power spectrum ratio	$PSR = \frac{P_0}{P} = \frac{\sum_{j=f_0-n}^{f_0+n} P_j}{\sum_{j=-\infty}^{\infty} P_j}$
34	VCF	Variance of central frequency	$VCF = \frac{1}{SM0}\sum_{j=1}^{M} P_j(f_j - f_c)^2 = \frac{SM2}{SM0} - \left(\frac{SM1}{SM0}\right)^2$

Sr. No.	Abv.	Name of Feature	Definition
35	AR1	Auto-regressive coefficients	$X_i = \sum_{p=1}^{p} a_p X_{i-p} + w_i$
36	AR2		
37	AR3		
38	AR4		p is order of the AR model, w_i is white noise error term

where X_i represents the EMG signal in a segment i and N denotes length of EMG signal, f_j is frequency of the spectrum at frequency bin j, P_j is the EMG power spectrum at frequency bin j and M is length of the frequency bin. UL, LL: upper and lower cut-off frequency of lower frequency band UH, LH: upper and lower cut-off frequency of upper frequency band.

ACKNOWLEDGMENT

The authors would like to thank Department of Electronics and Information Technology (DeitY), Government of India to provide the fellowship and Director, Thapar University, Patiala for constant encouragement for research work.

REFERENCES

[1] O. R. Jimenez-Fabian, Verlinden, "Medical Engineering & Physics Review of control algorithms for robotic ankle systems in lower-limb orthoses , prostheses , and exoskeletons ☪," *Med. Eng. Phys.*, vol. 34, no. 4, pp. 397–408, 2012.

[2] K. Veer, "A flexible approach for segregating physiological signals," *Meas. J. Int. Meas. Confed.*, vol. 87, pp. 21-26, 2016.

[3] H. S. Ryait, A. S. Arora, and R. Agarwal, "Interpretations of wrist/grip operations from SEMG signals at different locations on arm," *IEEE Trans. Biomed. Circuits Syst.*, vol. 4, no. 2, pp. 101–111, 2010.

[4] P. Geethanjali and K. K. Ray, "A Low-Cost Real-Time Research Platform for EMG Pattern Recognition-Based Prosthetic Hand," *IEEE/ASME Trans. Mechatronics*, vol. 20, no. 4, pp. 1948–1955, 2014.

[5] E. L. Mercado-Medina, Z. D. Chavarro-Hernandez, J. A. Dominguez-Jimenez, and S. H. Contreras-Ortiz, "Design of an electronic system for monitoring muscle activity in weight-lifting," in *2014 III International Congress of Engineering Mechatronics and Automation (CIIMA)*, 2014, pp. 1–4.

[6] M. S. Al-Quraishi, A. J. Ishak, S. A. Ahmad, and M. K. Hasan, "Multichannel EMG data acquisition system: Design and temporal analysis during human ankle joint movements," in *IECBES 2014, Conference Proceedings - 2014 IEEE Conference on Biomedical Engineering and Sciences: "Miri, Where Engineering in Medicine and Biology and Humanity Meet,"* 2015, no. December, pp. 338–342.

[7] F. N. Guerrero, E. M. Spinelli, and M. A. Haberman, "Analysis and Simple Circuit Design of Double Differential EMG Active Electrode," *IEEE Trans. Biomed. Circuits Syst.*, vol. 10, no. 3, pp. 787–795, 2016.

[8] A. Chatterjee, S. Gupta, S. Kumar, K. Garg, and A. Kumar, "An innovative device for instant measurement of Surface Electro-Myography for clinical use," *Meas. J. Int. Meas. Confed.*, vol. 45, no. 7, pp. 1893–1901, 2012.

[9] A. Phinyomark, P. Phukpattaranont, and C. Limsakul, "Expert Systems with Applications Feature reduction and selection for EMG signal classification," *Expert Syst. Appl.*, vol. 39, no. 8, pp. 7420–7431, 2012.

[10] K. Veer, T. Sharma, and R. Agarwal, "A neural network-based electromyography motion classifier for upper limb activities," *J. Innov. Opt. Health Sci.*, vol. 9, no. 6, pp. 1–8, 2016.

[11] D. Joshi and M. E. Hahn, "Terrain and Direction Classification of Locomotion Transitions Using Neuromuscular and Mechanical Input," *Ann. Biomed. Eng.*, vol. 44, no. 4, pp. 1275–1284, 2016.

[12] D. Farina et al., "The Extraction of Neural Information from the Surface EMG for the Control of Upper-Limb Prostheses: Emerging Avenues and Challenges," *IEEE Trans. Neural Syst. Rehabil. Eng.*, vol. 22, no. 4, pp. 797–809, 2014.

[13] J. D. Miller, M. S. Beazer, and M. E. Hahn, "Myoelectric walking mode classification for transtibial amputees," *IEEE Trans. Biomed. Eng.*, vol. 60, no. 10, pp. 2745–2750, 2013.

[14] K. Veer and R. Agarwal, "Wavelet denoising and evaluation of electromyogram signal using statistical algorithm," *Int. J. Biomed. Eng. Technol.*, vol. 16, no. 4, pp. 293–305, 2014.

[15] A. Alkan and M. Günay, "Expert Systems with Applications Identification of EMG signals using discriminant analysis and SVM classifier," *Expert Syst. Appl.*, vol. 39, no. 1, pp. 44–47, 2012.

[16] A. J. Young, S. Member, A. M. Simon, N. P. Fey, and L. J. Hargrove, "Classifying the Intent of Novel Users During Human Locomotion Using Powered Lower Limb Prostheses," in *Annual International IEEE EMBS Conference on Neural Engineering*, 2013, pp. 6–8.

[17] A. Phinyomark, A. Nuidod, P. Phukpattaranont, and C. Limsakul, "Feature Extraction and Reduction of Wavelet Transform Coefficients for EMG Pattern Classification," vol. 6, no. 6, 2012.

[18] A. Fougner, Ø. Stavdahl, P. J. Kyberd, Y. G. Losier, and P. A. Parker, "Control of Upper Limb Prostheses: Terminology and Proportional Myoelectric Control — A Review," vol. 20, no. 5, pp. 663–677, 2012.

[19] A. J. Young, A. M. Simon, N. P. Eey, and L. J. Hargrove, "Intent Recognition in a Powered Lower Limb Prosthesis Using Time History Information," *Ann. Biomed. Eng.*, vol. 42, no. 3, pp. 631–641, 2014.

[20] B. Chen et al., "Locomotion Mode Classification Using a Wearable Capacitive Sensing System," vol. 21, no. 5, pp. 744–755, 2013.

[21] A. J. Young, A. M. Simon, and L. J. Hargrove, "A Training Method for Locomotion Mode Prediction Using Powered Lower Limb Prostheses," *IEEE Trans. Neural Syst. Rehabil. Eng.*, vol. 22, no. 3, pp. 671–677, 2014.

[22] B. Chen, X. Wang, Y. Huang, K. Wei, and Q. Wang, "A foot-wearable interface for locomotion mode recognition based on discrete contact force distribution," *Mechatronics*, vol. 32, pp. 12–21, 2015.

[23] K. Yuan, Q. Wang, and L. Wang, "Fuzzy-Logic-Based Terrain Identification with Multisensor Fusion for Transtibial Amputees," *IEEE Trans. Mechatronics*, vol. 20, no. 2, pp. 618–630, 2015.

[24] A. J. Young and L. J. Hargrove, "A Classification Method for User - Independent Intent Recognition for Transfemoral Amputees using Powered Lower Limb Prostheses," vol. 24, no. 2, pp. 217–225, 2016.

[25] S. Pati, D. Joshi, and A. Mishra, "Locomotion classification using EMG signal," in *2010 International Conference on Information and Emerging Technologies*, 2010, pp. 1–6.

[26] H. Huang, F. Zhang, Y. L. Sun, and H. He, "Design of a robust EMG sensing interface for pattern classification," *J. Neural Eng.*, vol. 7, no. 5, p. 56005, 2010.

[27] T. A. ; K. I. ; G. W. ; A. B. Wright;, "A Method for Locomotion Mode Identification Using Muscle Synergies," *IEEE Trans. Neural Syst. Rehabil. Eng.*, vol. PP, no. 99, pp. 1–10, 2016.

[28] M. T. Farrell and H. Herr, "A method to determine the optimal features for control of a powered lower-limb prostheses," in *33rd Annual International Conference of the IEEE EMBS*, 2011, pp. 6041–6046.

[29] X. Zhang, D. Wang, Q. Yang, and H. Huang, "An Automatic and User-Driven Training Method for Locomotion Mode Recognition for Artificial Leg Control," in *34th Annual International Conference of the IEEE EMBS*, 2012, pp. 6116–6119.

[30] L. Du, F. Zhang, M. Liu, and H. Huang, "Toward Design of an Environment-Aware Adaptive Locomotion-Mode-Recognition System," *IEEE Trans. Biomed. Eng.*, vol. 59, no. 10, pp. 2716–2725, 2012.

[31] F. Zhang and H. Huang, "Source Selection for Real-Time User Intent Recognition Toward Volitional Control of Artificial Legs," *IEEE J. Biomed. Heal. Informatics*, vol. 17, no. 5, pp. 907–914, 2013.

[32] M. Liu, D. Wang, and H. H. Huang, "Development of an Environment-aware Locomotion Mode Recognition System for Powered Lower Limb Prostheses," *IEEE Trans. Neural Syst. Rehabil. Eng.*, vol. 24, no. 4, pp. 434–443, 2016.

[33] J. A. Spanias, A. M. Simon, K. A. Ingraham, and L. J. Hargrove, "Effect of Additional Mechanical Sensor Data on an EMG - based Pattern Recognition System for a Powered Leg Prosthesis," in *IEEE EMBS Conference on Neural Engineering*, 2015, pp. 22–24.

[34] M. E. Joshi, D., Hahn, "Terrain and Direction Classification of Locomotion Transitions Using Neuromuscular and Mechanical Input," *Ann. Biomed. Eng.*, vol. 44, no. 4, pp. 1275–1284, 2016.

[35] S. Pancholi, "Development of low cost EMG data acquisition system for Arm Activities Recognition," in *Intl. Conference on Advances in Computing, Communications and Informatics*, 2016, pp. 2465–2469.

[36] T. Instruments and I. Snas, "ADS1293 Low-Power, 3-Channel, 24-Bit Analog Front-End for Biopotential Measurements," 2014.

[37] R. N. Khushaba, A. Al-Timemy, S. Kodagoda, and K. Nazarpour, "Combined influence of forearm orientation and muscular contraction on EMG pattern recognition," *Expert Syst. Appl.*, vol. 61, pp. 154–161, 2016.
[38] Z. Li, B. Wang, C. Yang, and Q. Xie, "Boosting-Based EMG Patterns Classification Scheme for Robustness Enhancement," *IEEE J. Biomed. Heal. INFORMATICS*, vol. 17, no. 3, pp. 545–552, 2013.
[39] J. Margarito, R. Helaoui, A. M. Bianchi, F. Sartor, and A. G. Bonomi, "User-independent recognition of sports activities from a single wrist-worn accelerometer: A template-matching-based approach," *IEEE Trans. Biomed. Eng.*, vol. 63, no. 4, pp. 788–796, 2016.
[40] G. Rasool, K. Iqbal, N. Bouaynaya, and G. White, "Real-time Task Discrimination for Myoelectric Control Employing Task-Specific Muscle Synergies," *IEEE Trans. Neural Syst. Rehabil. Eng.*, vol. 4320, no. c, pp. 1–10, 2015.
[41] D. Yang, J. Zhao, Y. Gu, L. Jiang, and H. Liu, "EMG Pattern Recognition and Grasping Force Estimation: Improvement to the Myocontrol of Multi-DOF Prosthetic Hands," pp. 516–521, 2009.
[42] H. Huang, F. Zhang, L. J. Hargrove, Z. Dou, D. R. Rogers, and K. B. Englehart, "Continuous Locomotion-Mode Identification for Prosthetic Legs Based on Neuromuscular – Mechanical Fusion," *IEEE Trans. Biomed. Eng.*, vol. 58, no. 10, pp. 2867–2875, 2011.
[43] E. N. Kamavuako, E. J. Scheme, K. B. Englehart, and A, "Determination of optimum threshold values for EMG time domain features; a multi-dataset investigation," *J. Neural Eng.*, vol. 13, no. 4, pp. 1–10, 2016.
[44] N. R. Hudgins, Bernard, Parker, Philip, Scott, "HuginsParker(1993) IEEEtransBME40(1)82-94.pdf," *IEEE Trans. Biomed. Eng.*, vol. 40, no. 1, pp. 82–94, 1993.
[45] Y.-C. Du, C.-H. Lin, L.-Y. Shyu, and T. Chen, "Portable hand motion classifier for multi-channel surface electromyography recognition using grey relational analysis," *Expert Syst. Appl.*, vol. 37, no. 6, pp. 4283–4291, 2010.